

Comparison of Resonant Inelastic X-Ray Scattering Spectra and Dielectric Loss Functions in Copper Oxides

Jungho Kim,¹ D. S. Ellis,¹ H. Zhang,¹ J. P. Hill,² F. C. Chou,^{3,*} T. Gog,⁴ D. Casa,⁴ and Young-June Kim^{1,†}

¹*Department of Physics, University of Toronto, Toronto, Ontario M5S 1A7, Canada*

²*Department of Condensed Matter Physics and Materials Science,
Brookhaven National Laboratory, Upton, New York 11973, USA*

³*Center for Materials Science and Engineering, MIT, Cambridge, Massachusetts 02139, USA*

⁴*XOR, Advanced Photon Source, Argonne National Laboratory, Argonne, Illinois 60439*

(Dated: February 3, 2022)

We report empirical comparisons of Cu K-edge indirect resonant inelastic x-ray scattering (RIXS) spectra, taken at the Brillouin zone center, with optical dielectric loss functions measured in a number of copper oxides. The RIXS data are obtained for Bi_2CuO_4 , CuGeO_3 , $\text{Sr}_2\text{Cu}_3\text{O}_4\text{Cl}_2$, La_2CuO_4 , and $\text{Sr}_2\text{CuO}_2\text{Cl}_2$, and analyzed by considering both incident and scattered photon resonances. An incident-energy-independent response function is then extracted. The dielectric loss functions, measured with spectroscopic ellipsometry, agree well with this RIXS response, especially in Bi_2CuO_4 and CuGeO_3 .

PACS numbers: 78.70.Ck, 78.20.-e, 71.45.-d

Since the pioneering study of NiO by Kao *et al.* [1], indirect resonant inelastic x-ray scattering (RIXS) [2, 3] in the hard x-ray regime has been regarded as a promising momentum-resolved spectroscopic tool for investigating charge excitations in solids [4, 5, 6]. A variety of systems, including nickelates [7, 8], manganites [9, 10] and cuprates [11, 12, 13, 14, 15, 16, 17, 18, 19], have been studied by K-edge RIXS, revealing new and interesting charge excitations. Despite these early experiments, further developments of this promising technique have been hindered by the lack of a systematic theoretical understanding. The RIXS cross-section is complicated because the resonant contribution in RIXS generally involves correlation between more than two particles [2, 5, 20]. To date, theoretical studies of the RIXS cross section have mostly been limited to model-dependent calculations based on small clusters [21, 22, 23, 24]. This is in contrast with the cross-section for non-resonant inelastic x-ray scattering (IXS) which measures the two-particle charge correlation function [25]. Although there have been a few attempts to empirically relate the RIXS cross-section to a calculable two-particle correlation function [2, 3, 10, 11, 16, 26], details of the incident and scattered photon resonances and the nature of the response function measured by RIXS remain unclear.

In this context, recent theoretical studies by Ament and coworkers are noteworthy [2, 3]. Working in the limits of a local, strong (or weak), and short-lived, core hole potential, they were able to show that, in these limits, the RIXS cross section can be factored into a resonant prefactor that depends on the incident and scattered photon energies, and the dynamic structure factor, $S(\mathbf{q}, \omega)$ [3]. This result has important implications for the interpretation of RIXS spectra, since this approach then suggests that with proper handling of the prefactor, RIXS can be considered as a weak probe that measures $S(\mathbf{q}, \omega)$. It is

therefore important to test whether this theory can be applied to real systems or not, and delineate any necessary conditions for the applicability of Ref. [3].

In this Letter, we report a systematic comparison of the RIXS spectra and the dielectric loss functions in various copper oxides: Bi_2CuO_4 , CuGeO_3 , $\text{Sr}_2\text{Cu}_3\text{O}_4\text{Cl}_2$, La_2CuO_4 , and $\text{Sr}_2\text{CuO}_2\text{Cl}_2$. We measured the RIXS spectrum of each sample at the Γ -position and extracted a response function that does not depend on the incident energy. This response function is compared with the optical dielectric loss function, measured using spectroscopic ellipsometry on the same sample. Dielectric loss function data from published electron energy loss spectroscopy (EELS) studies are also used to augment the optical data. We show that overall energy loss-dependence of the RIXS response function is in good agreement with the optical dielectric loss function over a wide energy range for all samples. In particular, the agreement is excellent for the local systems Bi_2CuO_4 and CuGeO_3 , suggesting that the RIXS response is intimately related to the dynamic structure factor and thus to the charge density-density correlation function in these materials. On the other hand, additional low-energy spectral features are observed for the corner-sharing two dimensional copper oxides such as La_2CuO_4 and $\text{Sr}_2\text{CuO}_2\text{Cl}_2$, indicating that non-local nature of intermediate states may play an important role in such compounds.

The Cu K-edge RIXS experiments were carried out at the 9IDB beamline at the Advanced Photon Source. Channel-cut Si(444)/Si(333) monochromators, various detector slits, and a diced Ge(733) analyzer with 1 m radius of curvature were utilized. The data shown here are obtained with low resolution (FWHM of the elastic line: 300 – 400 meV) unless otherwise specified. The single crystal samples of Bi_2CuO_4 , CuGeO_3 , La_2CuO_4 were grown using the traveling solvent floating zone method,

TABLE I: Summary of the experimental conditions and fitting parameters for the samples studied. Energies are in units of eV. Note that the CuGeO_3 data were taken at the 1D zone center of the chain.

Sample	Q (rlu)	polarization	ω_{res}	Γ	$ U $	T (K)
Bi_2CuO_4	(0,0,3)	$\epsilon \perp z$	8993.7	3.2	5.7	20
CuGeO_3	(1.5,0,0)	$\epsilon \sim \parallel z^a$	8985.7	2.5	4.3	300
$\text{Sr}_2\text{Cu}_3\text{O}_4\text{Cl}_2$	(0,0,9)	$\epsilon \perp z$	8989.0	3.5	4.5	300
La_2CuO_4	(3,0,0)	$\epsilon \parallel z$	8989.3	2.5	2.5	20
$\text{Sr}_2\text{CuO}_2\text{Cl}_2$	(0,0,11)	$\epsilon \perp z$	8992.4	3.0	2.6	300

^aThe polarization was along the crystallographic b-direction.

while the $\text{Sr}_2\text{Cu}_3\text{O}_4\text{Cl}_2$ and $\text{Sr}_2\text{CuO}_2\text{Cl}_2$ single crystals were prepared using the CuO flux method. The experimental conditions for each measurement are summarized in Table I. All RIXS measurements were carried out at the appropriate $\mathbf{q}=0$ reciprocal space positions. We have also studied the optical properties of the same samples with spectroscopic ellipsometry using a VASE (Woollam) ellipsometer. The real and imaginary part of the dielectric function were obtained from 1 eV to 6.2 eV at room temperature [27].

From the Eq. (26) in Ref. [3], the RIXS intensity $I(\omega, \omega_i)$ at $\mathbf{q}=0$ can be written as [28]

$$I \sim P(\omega, \omega_i) S(\omega) \delta(\omega - \omega_s + \omega_i), \quad (1)$$

where ω_i and ω_s are the incident and scattered photon energies, respectively, and $\omega = \omega_i - \omega_s$ is the energy loss. Here, $S(\omega) \equiv S(\mathbf{q} = \mathbf{0}, \omega)$ is the density response function at $\mathbf{q} = \mathbf{0}$ [5, 11]. Note that the resonance behavior involving intermediate states is all contained in the prefactor $P(\omega, \omega_i) = [(\omega_s - \omega_{res})^2 + \Gamma^2]^{-1} [(\omega_i - \omega_{res} - |U|)^2 + \Gamma^2]^{-1}$, which consists of two Lorentzian functions with damping (Γ) due to the finite lifetime of intermediate states. Each of these Lorentzian functions represent resonant behavior of incident and scattered photons, resonating at $\omega_{res} + |U|$ and ω_{res} , respectively, where $|U|$ is the local core hole potential.

We have analyzed our data by fitting all scans using Eq. (1), leaving ω_{res} , Γ , and the overall amplitude as free parameters. The fitting parameters for each sample are listed in Table I. Note that the peak position of the K-edge x-ray absorption spectrum (ω_{XAS}) is taken to be the incident photon resonance energy $\omega_{res} + |U|$. Since the incident photon energy ω_i is fixed for each scan, the $[(\omega_i - \omega_{XAS})^2 + \Gamma^2]^{-1}$ factor becomes a constant for each scan, leaving a single Lorentzian function in the prefactor. This remaining Lorentzian function centered at ω_{res} with width Γ describes the scattered photon resonance, which is necessary to obtain satisfactory fits [29].

In order to illustrate the use of the scattered photon resonance, the RIXS spectra of CuGeO_3 obtained with four different incident energies are plotted as a function of ω_s in Fig. 1(a). For each scan, there are two strong

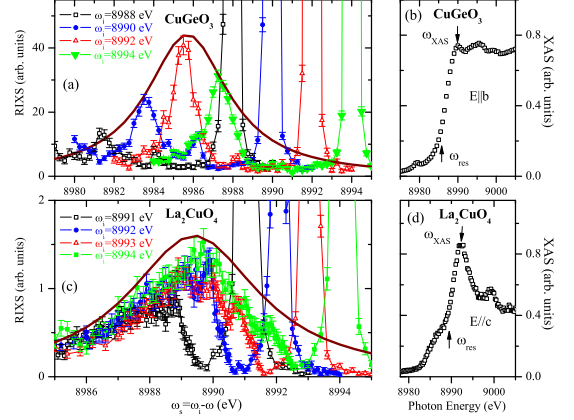


FIG. 1: (Color online) (a) The K-edge RIXS spectra taken with four incident photon energies as a function of the scattered photon energy (ω_s) for CuGeO_3 . Note that the inelastic intensity follows an envelope function (solid line), indicating the scattered photon resonance. (b) The total fluorescence yield obtained near the Cu K-edge for CuGeO_3 . Two resonance energies, ω_{XAS} and ω_{res} , are noted. Similar plots for La_2CuO_4 are shown in (c) and (d). The RIXS data for La_2CuO_4 are taken from Ref. [15].

energy loss features centered at $\omega = 3.8$ eV and 6.5 eV. Although the energy-loss positions of these features do not change from scan to scan, the ratio between these two features varies quite a lot. The $\omega = 6.5$ eV peak is strongest when $\omega_i = 8992$ eV, while the $\omega = 3.8$ eV peak is strongest when $\omega_i = 8990$ eV. These observations seem to suggest that the energy loss is a material-specific property arising from $S(\omega)$, while the intensity variation is due to the resonance prefactor. The scattered photon resonant prefactor, shown as the Lorentzian envelope function in Fig. 1(a), describes the intensity ratio variation between these two peaks very well. In other words, by fitting all our data to Eq. (1), it is possible to extract an ω_i -independent part of the spectrum: $S(\omega)$.

Similar analysis of the ω_i and ω_s dependence of the spectra has also been carried out for the other samples. The data for La_2CuO_4 are shown in Fig. 1(c)-(d). Again the envelope function seems to describe the intensity variation as a function of ω_i well. In Fig. 2(a)-(e), the resulting $S(\omega)$ spectra are shown as a function of ω . The elastic tail in the RIXS raw data are fitted to a Lorentzian function and subtracted in this plot. We find that, for a given material, the spectra obtained with different incident energies collapse onto a single spectrum that represents $S(\omega)$, as expected. We note that a similar analysis was carried out in Refs. [11, 34, 35], but with the assumption that the incident and scattered intermediate states were degenerate ($U = 0$) [11, 34] or nearly degenerate ($|U| = 1$ eV) [35]. One could take the same approach here, but we found that assuming two distinct intermediate states for ω_i and ω_s is essential in describ-

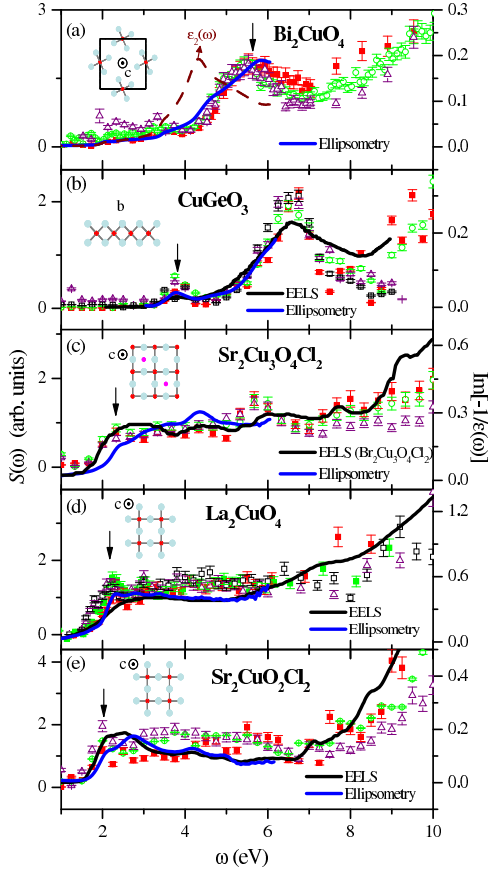


FIG. 2: (Color online) Comparison of $S(\omega)$ with the measured $\text{Im}(-1/\epsilon(\omega))$ for various cuprates. Different symbols are used to denote RIXS spectra obtained with different incident energies. These incident photon energies are (a) 8997.5 – 8999.5 eV; (b) 8988 – 8994 eV; (c) 8992 – 8994 eV; (d) 8991 – 8994 eV; and (e) 8993 – 8995 eV. The EELS data for CuGeO_3 , La_2CuO_4 , and $\text{Sr}_2\text{CuO}_2\text{Cl}_2$ are taken from Refs. [30], [31], and [32], respectively. Although there is no EELS spectrum for $\text{Sr}_2\text{Cu}_3\text{O}_4\text{Cl}_2$ available in the literature, that of $\text{Ba}_2\text{Cu}_3\text{O}_4\text{Cl}_2$ is shown [33].

ing all the spectral features simultaneously. As discussed in Ref. [3], these two resonances come from the intermediate state energies separated by the core hole potential. Table I lists the values of ω_{res} obtained from our fitting and $|U| = \omega_{XAS} - \omega_{res}$. It should be noted that $|U| < \Gamma$ for La_2CuO_4 and $\text{Sr}_2\text{CuO}_2\text{Cl}_2$.

Next, we compare the extracted $S(\omega)$ with the measured optical response functions. One of the key results in Ref. [3] is that apart from the prefactor, the RIXS should measure $S(\omega)$, which captures the physics of the valence electron system. Several studies have also argued that the response function of RIXS corresponds to the dynamic structure factor, $S(\mathbf{q}, \omega)$, or equivalently the dielectric loss-function, $\text{Im}(-1/\epsilon(\omega))$ [2, 3, 10, 11, 16, 26]. Having obtained an incident-energy-independent RIXS response function, we are now in a position to test this idea directly. To do so, we obtained optical spectra from

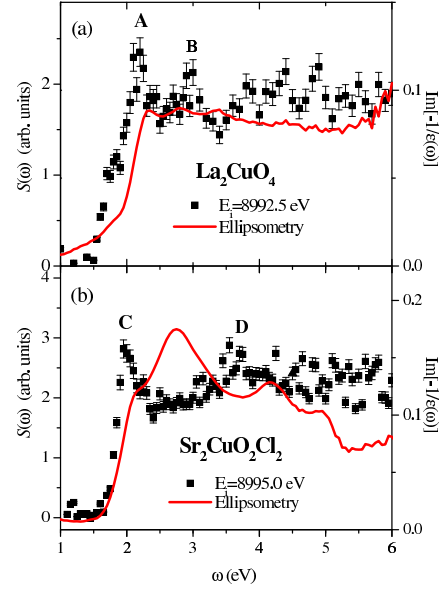


FIG. 3: (Color online) The function $S(\omega)$ extracted from high-resolution RIXS data and compared with $\text{Im}(-1/\epsilon(\omega))$ for (a) La_2CuO_4 and (b) $\text{Sr}_2\text{CuO}_2\text{Cl}_2$.

ellipsometry measurements on the same samples used in the RIXS experiments. As a first comparison, we plot both the imaginary part of complex dielectric function, $\epsilon_2(\omega)$, and $\text{Im}(-1/\epsilon(\omega))$ in Fig. 2(a). It is clear that $S(\omega)$ is most similar to $\text{Im}(-1/\epsilon(\omega))$, but not to $\epsilon_2(\omega)$. In Fig. 2, measured $\text{Im}(-1/\epsilon(\omega))$ spectra for the other systems are overlaid with the $S(\omega)$ spectra. We also include the available EELS spectra near $\mathbf{q} = 0$ from the literature [30, 31, 32, 33]. It is well known that EELS at $\mathbf{q} = 0$ also measures $\text{Im}(-1/\epsilon(\omega))$. Note that the RIXS data are plotted using an arbitrary vertical scaling in making these comparison.

Figure 2 shows that the extracted $S(\omega)$ is in good overall agreement with the general shape of $\text{Im}(-1/\epsilon(\omega))$ for all five systems studied, regardless of the detailed characteristics of the particular charge excitations. In particular, Bi_2CuO_4 and CuGeO_3 show excellent agreement in terms of the number of peaks and their positions. In the other systems, however, it is not easy to see a one-to-one correspondence with particular features, in part because the spectra themselves are more complex with several features in the low energy region. These will be discussed in more detail later. Nevertheless, as indicated by the arrows in Fig. 2(c)-(e), the position of the insulating gap and the increase in $S(\omega)$ above 7 ~ 8 eV agree reasonably well for the two data sets.

To make a detailed comparison for La_2CuO_4 and $\text{Sr}_2\text{CuO}_2\text{Cl}_2$, we plot high-resolution (~ 130 meV) RIXS data and ellipsometry data for these two materials in Fig. 3 focusing on the low energy region. The high-resolution $S(\omega)$ is obtained via the same procedure as described above, with the same parameters. Features la-

beled A and C in the two RIXS spectra correspond to the lowest energy charge excitations, and presumably have the same origin as the charge gap in $\text{Im}(-1/\varepsilon(\omega))$, yet their spectral shape appears different for the two techniques. We also observe an additional peak, B, around 3 eV, in La_2CuO_4 , which is not apparent in the ellipsometry data. Similarly, feature D in $\text{Sr}_2\text{CuO}_2\text{Cl}_2$ is not observed in the ellipsometry, while strong features are observed between C and D. In the case of La_2CuO_4 , $S(\omega)$ has a small peak below A which is due to a d-d excitation [36]. The d-d excitation also shows up in ellipsometry data, though its spectral weight is suppressed.

In order to understand the observed discrepancy, it is useful to consider the structural differences between the cuprate samples studied here. Although the main structural building block in all these samples is a plaquette composed of one Cu and four oxygens, the network formed by these CuO_4 plaquettes is very different, as shown in Fig. 2 insets. In Bi_2CuO_4 , these plaquettes are isolated, while they form an edge-sharing chain in CuGeO_3 . On the other hand, the plaquettes form a two-dimensional corner-sharing network in the other three compounds. It is important to realize that the interaction between the valence electron system and the 1s core hole in the intermediate state is *non-local* in the case of such corner-sharing copper oxides due to the 180 degree Cu-O-Cu bond in these compounds [37, 38]. Therefore, one can imagine that the local core hole potential approximation used in Ref. [3] may break down in this case. The importance of non-locality can also be inferred from the cluster calculation [39], in which a cluster substantially larger than the plaquette was necessary to explain the observed XAS spectrum in La_2CuO_4 .

We note that in their study of $\text{HgBa}_2\text{CuO}_{4+\delta}$, Lu et al. reported that RIXS reveals more excitations than conventional two-particle spectroscopy such as optical spectroscopy [14]. In addition, RIXS experiments on La_2CuO_4 have shown that there are many charge excitation peaks in addition to the lowest 2 eV peak [7, 15, 36]. The observed fine structure, such as the features B and D in Fig. 3, thus could arise from the difference in the matrix elements that enhances certain spectral features selectively.

In summary, we show that overall spectral features of the *indirect* resonant inelastic x-ray scattering response function are in a reasonable agreement with the optical dielectric loss function over a wide energy range. In the case of Bi_2CuO_4 and CuGeO_3 , we observe that the incident energy independent response function, $S(\mathbf{q} = \mathbf{0}, \omega)$, matches very well with the dielectric loss function, $\text{Im}(-1/\varepsilon(\omega))$, suggesting that the local core hole approximation treatment of Ref. [3] works well in these compounds. We also find that corner-sharing two dimensional copper oxides exhibit more complex excitation features than those observed in the dielectric loss functions. Our study seems to suggest that one can probe two-particle charge

correlation function with indirect resonant inelastic x-ray scattering.

We would like to thank Luuk Ament, Fiona Forte, and J. van den Brink for the discussions. Research at the University of Toronto was supported by the NSERC of Canada, Canadian Foundation for Innovation, and Ontario Ministry of Research and Innovation. Work at Brookhaven was supported by the U. S. DOE, Office of Science Contract No. DE-AC02-98CH10886. Use of the Advanced Photon Source was supported by the U. S. DOE, Office of Science, Office of Basic Energy Sciences, under Contract No. W-31-109-ENG-38.

* Present Address: Center for Condensed Matter Sciences, National Taiwan University, Taipei 10717, Taiwan.

† Electronic address: yjkim@physics.utoronto.ca

- [1] C. C. Kao, et al., Phys. Rev. B **54**, 16361 (1996).
- [2] J. van den Brink and M. A. van Veenendaal, Europhys. Lett. **73**, 121 (2006).
- [3] L. J. P. Ament, et al., Phys. Rev. B **75**, 115118 (2007).
- [4] A. Kotani and S. Shin, Rev. Mod. Phys. **73**, 203 (2001).
- [5] P. M. Platzman and E. D. Isaacs, Phys. Rev. B **57**, 11107 (1998).
- [6] J. P. Hill, et al., Phys. Rev. Lett. **80**, 4967 (1998).
- [7] E. Collart, et al., Phys. Rev. Lett. **96**, 157004 (2006).
- [8] S. Wakimoto, et al., unpublished, arXiv:0806.3302.
- [9] T. Inami, et al., Phys. Rev. B **67**, 045108 (2003).
- [10] S. Grenier, et al., Phys. Rev. Lett. **94**, 047203 (2005).
- [11] P. Abbamonte, et al., Phys. Rev. Lett. **83**, 860 (1999).
- [12] M. Z. Hasan, et al., Science **288**, 1811 (2000).
- [13] S. Suga, et al., Phys. Rev. B **72**, 081101(R) (2005).
- [14] L. Lu, et al., Phys. Rev. Lett. **95**, 217003 (2005).
- [15] Y. J. Kim, et al., Phys. Rev. Lett. **89**, 177003 (2002).
- [16] Y. J. Kim, et al., Phys. Rev. Lett. **92**, 137402 (2004).
- [17] K. Ishii, et al., Phys. Rev. Lett. **94**, 187002 (2005).
- [18] K. Ishii, et al., Phys. Rev. Lett. **94**, 207003 (2005).
- [19] J. P. Hill, et al., Phys. Rev. Lett. **100**, 097001 (2008).
- [20] T. P. Devereaux and R. Hackl, Rev. Mod. Phys. **79**, 3705 (2007).
- [21] K. Tsutsui, et al., Phys. Rev. Lett. **83**, 3705 (1999).
- [22] T. Nomura and J. I. Igarashi, Phys. Rev. B **71**, 035110 (2005).
- [23] R. S. Markiewicz and A. Bansil, Phys. Rev. Lett. **96**, 107005 (pages 4) (2006).
- [24] F. Vernay, et al., Phys. Rev. B **77**, 104519 (pages 10) (2008).
- [25] P. M. Platzman and P. A. Wolf, *Waves and Interactions in solid state plasmas* (Academic Press, New York, 1973).
- [26] Y.-J. Kim, et al., Phys. Rev. B **76**, 155116 (2007).
- [27] For $\text{Sr}_2\text{Cu}_3\text{O}_4\text{Cl}_2$ and $\text{Sr}_2\text{CuO}_2\text{Cl}_2$, the pseudo dielectric functions were taken due to their planar surfaces.
- [28] We use the spinless fermion expression from Ref. [3], since double occupancy can be ignored in these copper oxide compounds due to the strong on-site Coulomb interaction. Note also that the energy notation used here is slightly different from that of Ref. [3].
- [29] We made the self-absorption correction for ω_s following the approach in Tröger et al., Phys. Rev. B **46**, 3283 (1992). We found that this correction has a negligible effect

within our statistics and energy resolution.

- [30] S. Atzkern, et al., Phys. Rev. B **64**, 075112 (2001).
- [31] M. Terauchi and M. Tanaka, Micron **30**, 371 (1999).
- [32] A. S. Moskvina, et al., Phys. Rev. B **65**, 180512(R) (2002).
- [33] O. Knauff, et al., J. Low Temp. Phys. **105**, 353 (1996).
- [34] G. Döring, et al., Phys. Rev. B **70**, 085115 (2004).
- [35] L. Lu, et al., Phys. Rev. B **74**, 224509 (2006).
- [36] D. S. Ellis, et al., Phys. Rev. B **77**, 060501(R) (2008).
- [37] M. A. van Veenendaal, et al., Phys. Rev. B **47**, 11462 (1993).
- [38] K. Okada and A. Kotani, Phys. Rev. B **52**, 4794 (1995).
- [39] C. Li, et al., Physica C **175**, 369 (1991).